

SAR and B1 Field in a Human Head Model for Birdcage, TEM and Microstrip Coils at 7T

C. Wang¹, Y. Pang¹, B. Wu¹, and G. X. Shen¹

¹Electrical and Electronic Engineering, The University of Hong Kong, Hong Kong, Hong Kong

Introduction:

The advantage of high field MRI is high SNR which can increase image resolution or decrease acquisition time. However, there are some challenges, such as the RF wavelength effect and the power deposition in tissues. A comparison of three different volume coils loaded with the same spherical homogeneous phantom has been reported [1]. In order to mimic the B_1 field distribution and SAR in a realistic human head, an anatomically accurate human head model was chosen for the comparison of Birdcage, TEM and Microstrip at 300MHz.

Methods:

Three volume coils, Birdcage, TEM and Microstrip at 300MHz were designed and modeled. All coils have identical length (21 cm) and inner diameter (26 cm). Each coil consists of 16 rungs. The shield diameters of Birdcage, TEM and Microstrip coils are 32cm, 32cm and 28cm respectively. Three identical capacitors were equally distributed at each rung of Birdcage coil. The same capacitors were also placed at the middle of each end ring segment for the Birdcage coil. The legs and the end rings of Birdcage are 10mm width. The cross section of each rung of TEM coil is 10mm x 10mm square and the strip width of Microstrip coil is 20mm. The finite-difference time-domain (FDTD) method is used to calculate the transient B_1 fields using XFDTD software (Remcom, Inc., State College, PA). These three volume coils were modeled with 5mm isotropic resolution. Copper was modeled as a conductor with conductivity of 5.95×10^7 S/m and capacitors were treated as passive loads. Tuning was performed by changing the capacitance for birdcage coil, by lengthening or shortening the inner conductors of the rungs for TEM and by changing the relative permittivity of dielectric materials for Microstrip coil. All these volume coils are tuned to 300MHz and driven in quadrature by two current sources. Two different samples, a spherical phantom and human head model are used for simulation. The spherical phantom has 18cm diameter which relative permittivity is 51.898 and conductivity is 0.553 S/m to represents average brain tissue at 300MHz. The home-made anatomically-accurate human head model was chosen from the Visible Human Project (National Library of Medicine, <http://www.brooks.af.mil/AFRL/HEAD/hedr/>). SAR was calculated after solving their electrical fields in the samples. Circularly-polarized components of the B_1 field (B_1^+ and B_1^-) were calculated from two sets of transient B_1 fields which are a quarter period apart in time[2][3].

Results and Discussion:

For comparison, the B_1^+ field magnitudes at the center of coils are normalized to 100%. When loaded with the spherical phantom, the percentages of sample on the central axial plane having a B_1^+ field magnitude within $\pm 20\%$ of that plane mean are 55%, 72% and 59% for shielded Birdcage, TEM and Microstrip volume coils respectively. The central axial planes in the modeled Birdcage, TEM and Microstrip volume coils loaded with the anatomically accurate human head model were shown in Fig. 1(top), and the B_1^+ field magnitudes on these central axial planes in the head model were shown in Fig.1 (bottom). Note that in Fig. 1(bottom), the B_1^+ field magnitudes outside the head model were truncated to zero. The dielectric resonance phenomenon is visible. The percentages of the samples on the central axial plane of the head model having a B_1^+ field magnitude within $\pm 20\%$ of the average B_1^+ field magnitude on that plane are 63%, 78% and 64% for Birdcage, TEM and Microstrip coils respectively. The results indicate that TEM coil has the best B_1^+ field homogeneity when loaded with the spherical phantom or the head model. Compared with the results by using the uniform spherical phantom, the B_1^+ field homogeneity in head model increases more than 5%. One of the reasons is that the dielectric effect in the spherical phantom is stronger than that in the head model. It may be caused by the complex tissues within the head model. Average SAR and maximum local SAR in the spherical phantom and the head model for Birdcage, TEM and microstrip volume coils are shown in Table 1. Microstrip volume coil has the lowest average SAR and the lowest maximum local SAR because its electric fields are mainly restricted between strip line and ground. Compared with the results by using spherical phantom, the average SAR in the head model is slightly higher than those in the spherical phantom and the maximum local SAR in the head model increase dramatically. The reason may lie in that there are some tissues having much higher conductivity in head model than the average brain tissue in the spherical phantom. The local SAR distributions on the central axial plane through head model for the RF coils were shown in Fig 2. The black holes at the anteriority of the head models in Fig 2 are areas of internal air. The local SAR at the periphery of brain is much higher than that in the middle of brain. It is caused by that the electric field at the periphery of head model is stronger than that in the middle of the head model.

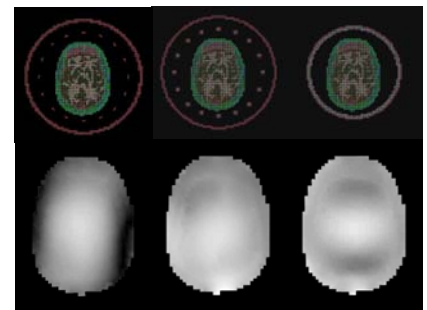
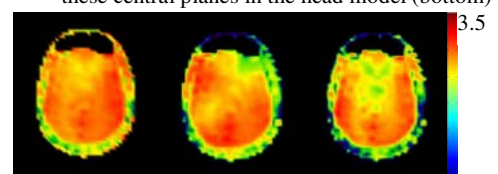


Fig. 1: The central axial planes in Birdcage, TEM and Microstrip coils loaded with the head model (top), and the normalized B_1^+ fields on these central planes in the head model (bottom)



Birdcage TEM Microstrip

Fig. 2: Local SAR distribution in the axial plane through head model within Birdcage, TEM and Microstrip coils. Values above maximum value in scale are represented with the same color

Spherical phantom / Head model	Birdcage	TEM	Microstrip
Average SAR(W/kg)	2.83 / 3.02	2.54 / 2.63	1.98 / 2.15
Max. Local SAR (W/kg)	6.13 / 53.6	5.82 / 45.4	3.49 / 32.3

Table 1: SAR normalized for a 5-ms 90° rectangular RF pulse with 50% duty cycle within the Spherical phantom / Head model for Birdcage, TEM and Microstrip coils

Acknowledgement:

This work was supported by RGC Grant 7045/01E, 7170/03E and 7168/04E.

References:

- [1] C. Wang, et al., 14th Proc. of ISMRM, p.3533, 2006
- [2] DI. Hoult, Concepts in Magn Reso. 12(4): 173-187, 2000
- [3] CM. Collins, et al., 7th Proc. of ISMRM, p.417, 1999